# Chapter 6. $NO_3$ Hydrogen-Abstraction from Aldehydes

## 6.1. Introduction

The consequences of the emission of aldehydes into the atmosphere or their formation in the troposphere from the decomposition or oxidation of other pollutants have been the object of several experimental and theoretical studies.[1] It is well known that during the daytime the photolysis of aldehydes and their reaction with OH radicals are the most probable processes.

The OH radical is the key species in the chemistry of the daytime troposphere. Since it is the most important oxidant, practically all organic and inorganic compounds are transformed by reaction with OH. The hydroxyl radical is formed mainly from three routes: the photolysis of $O_3$ and HONO, and from the reaction between $HO_2$ and NO (the most important source under noon-time conditions). In the absence of sunlight the OH radical concentration in the troposphere is very low.[2]

Numerous studies of the reaction of OH with aldehydes have been performed, both experimentally and theoretically.[3,4] Very recent theoretical studies[5] showed the importance of considering the formation of a reactant complex in the kinetics of the OH hydrogen-abstraction reaction from a series of aldehydes (XCHO: X = F, Cl, H, $CH_3$) at the level of theory chosen (geometries and energies were calculated at the MP2(FC) and CCSD(T) levels of theory, respectively, using the 6-311++G(d,p) basis set). The importance of aldehydes in the chemistry of the polluted atmosphere has been explained elsewhere.[3,5,6] TST[7] was applied successfully in the calculation of the rate constants. These calculations considered a complex mechanism in which the overall rate depends on the rates of two competitive reactions: a reversible step where a reactant complex is formed, followed by the irreversible hydrogen abstraction to form the products. Tunneling corrections were incorporated assuming an unsymmetrical Eckart barrier.[8]

Nitrate radicals were first detected in the stratosphere in 1978[9] and two years later were observed in the troposphere.[10] This free radical, as well as the OH radical, is a strong oxidizing agent and reacts with a number of atmospheric species.[11] The reaction of $NO_3$ radicals with atmospheric organic molecules can lead to the formation of undesirable compounds such as: $HNO_3$,[12] peroxyacyl nitrates (PANs)[13] and dinitrates.[14] The only primary source of $NO_3$ in the troposphere requires the simultaneous presence of $NO_2$ and $O_3$ in the same airmass, but during the daytime $NO_3$ radicals photolize rapidly, thus its presence in the troposphere is only significant at night. Measurements made over the past 15 years show nighttime $NO_3$ concentrations near ground level over continental areas ranging up to $1.7 \cdot 10^{-4}$ mol $L^{-1}$ ($1.0 \cdot 10^{10}$ molecule $cm^{-3}$).

At night, $NO_3$ radicals play the same role as do OH radicals during the day.[15] Thus we should expect the reaction with $NO_3$ radicals to be an important nighttime tropospheric removal route for aldehydes, as has already been mentioned elsewhere.[16] The reaction of $NO_3$ radicals with unsaturated organic compounds (alkenes, halogenated alkenes, alcohols, terpenes) is also known to represent an important sink for these species in the nighttime troposphere, and a number of experimental and theoretical studies have been performed in this direction.[17] Experimental studies on the reaction between alkanes, aliphatic alcohols and ethers with $NO_3$ radicals have also been performed.[14,18]

There have been fewer kinetic studies on the reactions of $NO_3$ with aldehydes than on the corresponding reactions with OH radicals. This situation may be due to the differences in the reactivities of these two oxidant radicals, among other factors, as discussed below. Several experimental kinetic studies on the reactions between $NO_3$ radicals and aliphatic aldehydes ($C_1$-$C_4$, and certain $C_5$ and $C_6$ aldehydes, among others)[16a,19] have been performed although most of the activation energies and Arrhenius pre-exponential factors have not been reported. According to the NIST chemical kinetics database, before the second half of 1998 the activation energy of the $NO_3$ reaction with $CH_3CHO$ was the only one determined. Rate constants have been reported for HCHO and $CH_3CHO$,[3a,b,c,20,21] but no kinetic data is available for FCHO and ClCHO. Furthermore,

no previous theoretical determinations of the kinetic parameters for $NO_3$ reactions with aldehydes have been published.

Due to the lack of kinetic information concerning the reaction of $NO_3$ with aldehydes, it was decided to extend the previous studies on the reactions with OH radicals to the $NO_3$ hydrogen-abstraction reactions with the same series of aldehydes:

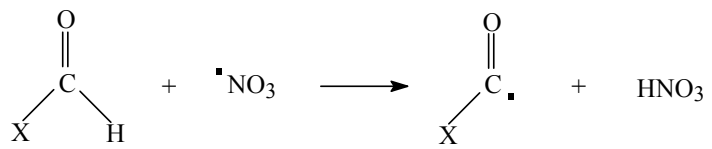


(XCHO: X = F, Cl, H, $CH_3$)

Previous calculations on the reaction of formaldehyde with OH[5a] show why the addition reaction of OH to the carbonylic double bond does not occur. Since the $NO_3$ radical is less reactive than the OH radical we should not expect the addition reaction of $NO_3$ to be of any importance. The abstraction mechanism has also been confirmed on the basis of the non-detection of $NO_2$ in the product mixture of the reaction and also because of the positive temperature dependence.[21b]

In the present study high-level *ab initio* calculations are performed to investigate the $NO_3$ hydrogen-abstraction reaction from FCHO, ClCHO, HCHO and $CH_3CHO$. In addition, TST is applied to the calculation of the rate constants and tunneling corrections are considered. The purpose of this study is to provide accurate theoretically determined kinetic parameters for these reactions.

## 6.2. Computational details

Geometries were optimized at the MP2(FC) and BH&HLYP[22] levels. Energies at the CCSD(T) level were calculated using the previous geometries and in all cases the 6-311G(d,p) basis set was used.

In Chapter 4,[5a] CCSD(T) energies obtained from MP2(FC) geometries using the 6-311++G(d,p) basis set were sufficient to reproduce experimental activation energies and rate constants for the reaction of OH radicals with HCHO and $CH_3CHO$. A later study on the HCHO + OH system,[23] that contains a comparative discussion on the performance of different levels of theory (MP2, MP4, B3LYP, BH&HLYP), showed that the CCSD(T)//MP2(FC) (the basis set will be omitted from this notation for simplicity) selection of methods gives the best results for this system and that the inclusion of diffuse functions on the hydrogen atoms does not change the results significantly. BH&HLYP, combined with a CCSD(T) single point calculation, works better for this system than the other hybrid DFT method, B3LYP. CCSD(T)//B3LYP barriers are too low, resulting in rate constants greater than expected. In addition, it should be mentioned that in previous studies[24] with DFT methods it was concluded that BH&HLYP is the best functional to characterize TS structures, vibrational frequencies and classical barrier heights for several reactions, including some hydrogen transfer processes. Furthermore, the addition of diffuse or polarization functions to the 6-311G(d,p) basis set has been shown to be unimportant.[24b] Therefore for the $NO_3$ reactions diffuse functions were not included in the basis set.

For reasons discussed below, the reactions were assumed to occur in a one-step mechanism:

$$XCHO + NO_3 \xrightarrow{k_D} XCO + HNO_3 \qquad (X = F, Cl, H, CH_3)$$

According to TST, the expression to calculate the direct rate constants, $k_D$, can be written as:

$$k_D = \kappa_D \frac{k_B T}{h} \frac{Q^{TS}}{Q^{React}} \exp\left(-\frac{\left(E^{TS} - E^{React}\right)}{RT}\right) \qquad (6.1)$$

The tunneling factor and $\Delta s_{½}$ were calculated by assuming an unsymmetrical Eckart barrier.

## 6.3. Results and discussion

### *6.3.1. The $NO_3$ radical*

There is a great deal of conflicting evidence both experimental and theoretical as to the ground electronic state and geometry of $NO_3$. While the experimental evidence[16b,25] suggests a $D_{3h}$ equilibrium ground state, quantum chemical studies are divided between $D_{3h}$[26] and $C_{2v}$[27] (or even $C_s$), depending on the applied method. Two $C_{2v}$ structures have been considered in the theoretical calculations and these have been previously denoted as 1L2S and 1S2L,[27b] according to the number of short (S) and long (L) NO bonds. Discrepancies between these predictions are partly due to the inherent difficulties of treating $NO_3$ properly, since it is an open-shell molecule with partial double bonds and low-lying excited electronic states.

Several CC calculations of different types have led to contradictory results for the $NO_3$ ground-state equilibrium geometry. A Fock space multireference CCSD (FSMR-CCSD) calculation yielded the symmetric $D_{3h}$ structure as the global minimum on the potential surface,[26g,h] whereas a quasirestricted Hartree-Fock CCSD (QHF-CCSD) calculation generated a $C_{2v}$ (1L2S) ground state;[27c] the same result was obtained with Brueckner orbitals.[27a] In contrast, by including triple excitations in single-point calculations, the global minimum was found to be of $D_{3h}$ symmetry.[26f]

A very interesting study on symmetry breaking and its effects on the potential surface of $NO_3$ was recently performed by Eisfeld and Morokuma.[26a] The authors refer to the symmetry breaking[28] of the electronic HF wavefunction as a problem frequently encountered in systems of high nuclear symmetry (see Section 2.5.2). This phenomenon leads to three different solutions for the ground electronic state of $NO_3$, corresponding to equilibrium geometries that are not connected on the same potential energy surface. Eisfeld and Morokuma's study concludes that the effective equilibrium geometry of the $NO_3$ radical is $D_{3h}$. Their calculations, performed at the MR-SDCI level with selected electronic configurations and an N-electron basis of CASSCF orbitals, showed that even CCSD and CCSD(T) cannot completely overcome the symmetry breaking of the

reference function and that three solutions with slightly different energies are obtained. Their study also confirmed previous observations[26f] about the inclusion of triplets in CC calculations.

It has been shown that spin-unprojected Møller-Plesset perturbation theory calculations (MP2 and MP4) predict the $NO_3$ ground state to be of $D_{3h}$ symmetry,[27b] although MP2 results still suffer from artifactual symmetry breaking since three different results are obtained.[26a]

In general, DFT methods have been reported to yield $D_{3h}$ symmetric densities and equilibrium geometries for the $NO_3$ radical.[26c,e,27b] A study by Sherrill *et al.*[26c] showed that DFT methods tend to avoid artifactual spatial symmetry breaking in the equilibrium geometry region even when unrestricted Hartree-Fock (UHF) fails. They also showed that the exchange functional seems to be more important than the correlation functional in determining whether or not a symmetry-broken solution is obtained, and that hybrid functionals which include large amounts of HF exchange lead to symmetry breaking.

The results obtained for the $NO_3$ radical at the levels of calculation employed in this work are listed in Table 6.1. At the MP2 level the $D_{3h}$ structure is the minimum, while at BH&HLYP level the $NO_3$ molecule prefers a $C_{2v}$ (1L2S) structure, the $D_{3h}$ structure being a saddle point of second order. With both geometries, the CCSD(T) single point calculation predicts the $D_{3h}$ structures to be of lower energy. The calculations on the $NO_3$ radical presented here are in agreement with the previous studies. The present study does not attempt to add new insight into the previous discussion about the $NO_3$ ground state symmetry. The above controversy will be used later in the chapter to justify the selection of computational methods.

Simple inspection of the reported activation energies and rate constants for the OH and $NO_3$ reactions from aldehydes shows that $NO_3$ is a less reactive molecule. This situation can be justified by analyzing the spin-density distribution in the radicals. In the $D_{3h}$ $NO_3$ molecule, the spin density is homogeneously distributed among the oxygen atoms, while

for the OH radical the spin density distribution is localized on oxygen. Another chemical reason to explain the smaller reactivity of the $NO_3$ radical can be found in its smaller hydrogen affinity, HA (see Table 6.2). The HA of $NO_3$ radicals is much smaller than that of OH, and not too much bigger than the HA of HCO and $CH_3CO$, radicals with which the $NO_3$ radicals have to compete.

**Table 6.1.** Calculations on the $NO_3$ radical at different levels of theory using the 6-311G(d,p) basis set. Atomic distances in Å, angles in degrees and energies in au.

| Geometry | MP2(FC) - $D_{3h}$ | MP2(FC) - $C_{2v}$ '1S2L' | MP2(FC) - $C_{2v}$ '1L2S' |
|---|---|---|---|
| $d(N,O^1)$ | 1.244 | 1.181 | 1.380 |
| $d(N,O^2)$, $d(N,O^3)$ | 1.244 | 1.247 | 1.204 |
| $\angle(O^1,N,O^2)$ | 120.0 | 127.0 | 113.6 |
| E(PMP2) | -279.66345 | -279.64122 | -279.62950 |
| E(CCSD(T)//MP2(FC)) | -279.66671 | -279.66367 | -279.66343 |
| NImag [(a)] | 0 | 0 | 0 |

| Geometry | BH&HLYP - $D_{3h}$ | BH&HLYP - $C_{2v}$ '1S2L' | BH&HLYP - $C_{2v}$ '1L2S' |
|---|---|---|---|
| $d(N,O^1)$ | 1.210 | 1.174 | 1.326 |
| $d(N,O^2)$ | 1.210 | 1.241 | 1.184 |
| $\angle(O^1,N,O^2)$ | 120.0 | 126.2 | 114.3 |
| E(BH&HLYP) | -280.12240 | -280.12821 | -280.13238 |
| E(CCSD(T)//BH&HLYP) | -279.66323 | -279.66297 | -279.66251 |
| NImag [(a)] | 2 | 1 | 0 |

[(a)] Number of imaginary frequencies

**Table 6.2.** Calculation of the hydrogen affinities (HA, in kJ/mol) of some radicals of interest at the PMP2 level using MP2(FC)/6-311++d(d,p) geometries.

| Radical (X) | HA [(a)] |
|---|---|
| OH | -508.2 |
| $NO_3$ | -389.5 |
| HCO | -368.1 |
| $CH_3CO$ | -371.8 |

[(a)] $HA_X = E_{HX} - (E_H + E_X)$

As a result of the lower reactivity of $NO_3$ radicals less stable reactant complexes and higher activation energies to form the TS are expected, compared to the results obtained for the analogous OH-aldehyde reactions.

### *6.3.2. **The reaction of $NO_3$ radicals with HCHO and $CH_3CHO$***

It is convenient to begin by explaining the selection of the best combination of methods that reproduce the experimental kinetics of the $NO_3$ hydrogen-abstraction reaction from $CH_3CHO$ and HCHO. The experimental rate constants, Arrhenius pre-exponential factors and activation energies are listed in Tables 6.3 ($CH_3CHO$ + $NO_3$) and 6.4 (HCHO + $NO_3$).

Previous calculations on the OH reaction with $CH_3CHO$[5a] showed that the abstraction of the aldehydic hydrogen atom is favoured. It has also been shown that the rate constant for the abstraction of one of the methyl hydrogen atoms is 10 times smaller.[3d] Since the $NO_3$ radicals are less reactive than the OH radicals, they should be more selective and the aldehydic hydrogen-abstraction should be the dominant process occurring in the reaction of $NO_3$ with $CH_3CHO$.

**Table 6.3.** Experimental kinetic results for the $NO_3$ reaction with $CH_3CHO$.

| Ref. (Year) | $E_a$ [(a)] | A [(b)] | k [(c)] | T (K) | P (atm) |
|---|---|---|---|---|---|
| 21a (2001) | 16.3 | - | $1.58 \cdot 10^6$ | 263 – 363 | 1 |
| 3a (1999) | 15.5 | $8.43 \cdot 10^8$ | $1.64 \cdot 10^6$ | 260 – 370 | [(d)] |
| 3b (1997) | 15.5 | $8.43 \cdot 10^8$ | $1.64 \cdot 10^6$ | 260 – 370 | [(d)] |
| 3c (1997) | 15.8 | $8.43 \cdot 10^8$ | $1.44 \cdot 10^6$ | 200 – 300 | [(d)] |
| 20a (1991) | 15.5 | $8.67 \cdot 10^8$ | $1.67 \cdot 10^6$ | 264 – 374 | [(d)] |
| 21b (1989) | 15.5 | $8.67 \cdot 10^8$ | $1.69 \cdot 10^6$ | 264 – 374 | [(e)] |
| 13a (1986) | - | - | $1.26 \cdot 10^6$ | 299 | 0.921 |
| 20d (1984) | - | - | $8.07 \cdot 10^5$ | 298 | 0.974 |
| 21c (1974) | - | - | $7.23 \cdot 10^5$ | 300 | 0.987 |

[(a)] kJ/mol; [(b)] L/mol·s; [(c)] At 298 K, in L/mol·s; [(d)] Literature review;
[(e)] 0.00132 – 0.00145 atm

Recently, a publication by D'Anna and coworkers[21a] reported the rate coefficient of the acetaldehyde reaction with $NO_3$ by the absolute rate fast-flow-discharge technique and by a relative method. They also optimized the TS of the aldehydic and methyl hydrogen-abstraction reactions at the MP2/cc-pVDZ level, although activation energies were not estimated theoretically. Their experimental and theoretical results point to the aldehydic hydrogen-abstraction as the only pathway for the $NO_3$ reaction with acetaldehyde under atmospheric conditions, in agreement with ideas derived from a previous work[16a] based on bond dissociation energies.

Energies obtained at different levels of theory were used to calculate the activation energy of the $CH_3CHO + NO_3$ reaction, and the values obtained are shown in Table 6.5,

along with the calculated reaction enthalpies, at 0 and 298 K. This is the only reaction among those studied for which activation energy values have been measured.

**Table 6.4.** Experimental kinetic results for the $NO_3$ reaction with HCHO.

| Ref. (Year) | $E_a$ [(a)] | A [(b)] | k [(c)] | T (K) | P (atm) |
|---|---|---|---|---|---|
| 3a (1999) | 20.2 [(d)] | $1.20 \cdot 10^9$ [(d)] | $3.49 \cdot 10^5$ | 298 | [(e)] |
| 3b (1997) | - | - | $3.49 \cdot 10^5$ | 298 | [(e)] |
| 3c (1997) | - | - | $3.49 \cdot 10^5$ | 298 | [(e)] |
| 20a (1991) | - | - | $3.49 \cdot 10^5$ | 298 | [(e)] |
| 20b (1988) | - | - | $3.25 \cdot 10^5$ | 295 | 0.974 |
| 20c (1985) | - | - | $3.79 \cdot 10^5$ | 298 | 0.921 |
| 20d (1984) | - | - | $1.95 \cdot 10^5$ | 298 | 0.974 |

[(a)] kJ/mol; [(b)] L/mol·s; [(c)] At 298 K, in L/mol·s; [(d)] Suggested in Ref. 3a(1999);
[(e)] Literature review

The PMP2 barrier is overestimated, as usual. This time the CCSD(T) calculation using MP2 geometries gives barriers that are still too high in comparison with experiment. The BH&HLYP and CCSD(T)//BH&HLYP barriers are too low. It is well known that DFT predicted barrier heights are often much lower than those obtained with *ab initio* methods.[29] In order to correct these last two barriers, an estimate of the magnitude of the basis set superposition error (BSSE)[30] was calculated by applying the counterpoise (CP) method[31] to the TS, following the original procedure in which the "monomeric units" (the reactants) upon forming the "intermolecular complex" (the TS) are not further optimized, *i.e.*, the "monomers" are frozen in their supermolecular geometries (see Section 2.3.2).

The BSSE was calculated using BH&HLYP as well as CCSD(T) (only for the $CH_3CHO$-$NO_3$ TS) energies, and are denoted BSSE(BH&H) and BSSE(CC), respectively. When

these two corrections are added to the CCSD(T)//BH&HLYP barrier, activation energies in good agreement with experiment are obtained.

**Table 6.5.** Activation energy ($E_a$) and reaction enthalpy ($\Delta H$), in kJ/mol, including zero-point (ZPE) or thermal vibrational corrections at 298.15 K (TCE), for the $NO_3$ hydrogen-abstraction reaction from $CH_3CHO$ at different levels of theory.

| Basis set: 6-311G(d,p) | $E_a^{(ZPE)}$ | $E_a^{(TCE)}$ | $\Delta H^{(ZPE)}$ | $\Delta H^{(TCE)}$ |
|---|---|---|---|---|
| PMP2 | 109.7 | 111.7 | -32.4 | -31.1 |
| CCSD(T)//MP2(FC) | 23.2 | 25.3 | -75.6 | -74.3 |
| BH&HLYP | -0.3 | 1.9 | -65.5 | -65.1 |
| CCSD(T)//BH&HLYP | 5.3 | 7.5 | -64.7 | -64.3 |
| BH&HLYP + BSSE(BH&H) | 6.9 | 9.1 | | |
| CCSD(T)//BH&HLYP + BSSE(BH&H) | 12.4 | 14.6 | | |
| CCSD(T)//BH&HLYP + BSSE(CC) | 18.8 | 21.0 | | |
| CCSD(T)//BH&HLYP* | 16.3 | 18.5 | -53.6 | -53.3 |
| Experiment | | 16.3 [(a)]<br>15.5 [(b)]<br>15.8 [(c)] | | -53.3 [(d)]<br>-67.3 [(e)] |

[(a)] Ref. 21a(2001); [(b)] Ref. 3a(1999), 3b(1997), 20a(1991), 21b(1989); [(c)] Ref. 3c(1997); [(d)] Ref. 3a(1999); [(e)] Ref. 3b(1997)

Bearing in mind the uncertainty about the ground state symmetry of the $NO_3$ radical, another correction to the CCSD(T)//BH&HLYP barrier is considered. Since the lowest CCSD(T) energy for $NO_3$ is obtained at the MP2(FC)-$D_{3h}$ geometry (see Table 6.1), this result was combined with the previous CCSD(T)//BH&HLYP calculations. That is, BH&HLYP geometries are used in the single point CCSD(T) calculations except for $NO_3$ for which the MP2(FC)-$D_{3h}$ structure is used. Frequency calculations are performed at the BH&HLYP level. Results using this correction will be denoted CCSD(T)//BH&HLYP* throughout the text. The activation energy obtained (16.3 at 0 K and 18.5 at 298 K, in

kJ/mol) is in very good agreement with experiment (15.5-16.3 kJ/mol). The reaction enthalpy calculated in this way is -53.6 at 0 K, and -53.3 at 298K (in kJ/mol), also in very good agreement with the latest experimental value (-53.3 kJ/mol).

For the HCHO + $NO_3$ reaction the calculated activation energies and reaction enthalpies are reported in Table 6.6, at 0 and 298 K. For this reaction an activation energy of 20.2 kJ/mol has been suggested by analogy with the reaction of $NO_3$ with $CH_3CHO$.[3a] The best results are once again obtained at the CCSD(T)//BH&HLYP level after considering the above mentioned corrections (CCSD(T)//BH&HLYP + BSSE(BH&H) and CCSD(T)//BH&HLYP*). The reaction enthalpy obtained at the CCSD(T)//BH&HLYP* level (-59.1 kJ/mol) is in excellent agreement with experiment as well (-57.1 kJ/mol).

**Table 6.6.** Activation energy ($E_a$) and reaction enthalpy ($\Delta H$), in kJ/mol, including zero-point (ZPE) or thermal vibrational corrections at 298.15 K (TCE), for the $NO_3$ hydrogen-abstraction reaction from HCHO at different levels of theory.

| Basis set: 6-311G(d,p) | $E_a^{(ZPE)}$ | $E_a^{(TCE)}$ | $E_{a\,(-1)}^{(ZPE)}$ | $E_{a\,(2)}^{(ZPE)}$ | $\Delta H^{(ZPE)}$ | $\Delta H^{(TCE)}$ |
|---|---|---|---|---|---|---|
| PMP2 | 118.2 | 119.3 | -70.0 | 48.2 | -41.2 | -40.2 |
| CCSD(T)//MP2(FC) | 32.4 | 33.6 | 10.7 | 43.2 | -81.1 | -80.1 |
| BH&HLYP | 3.2 | 3.9 | 5.1 | 8.3 | -70.1 | -70.0 |
| CCSD(T)//BH&HLYP | 11.3 | 12.0 | 6.7 | 18.0 | -70.3 | -70.2 |
| BH&HLYP + BSSE(BH&H) | 10.2 | 10.9 | | | | |
| CCSD(T)//BH&HLYP + BSSE(BH&H) | 18.3 | 19.0 | | | | |
| CCSD(T)//BH&HLYP* | 22.4 | 23.1 | -4.4 | 18.0 | -59.3 | -59.1 |
| Experiment | | 20.2 [(a)] | | | | -57.1 [(b)]<br>-58.4 [(c)] |

[(a)] Suggested in Ref. 3a(1999), 3b(1997); [(b)] Ref. 3a(1999); [(c)] Ref. 3b(1997)

The values of the partition functions needed for the calculation of the TST rate constants of the reactions studied at MP2 and BH&HLYP levels of theory are given in Tables 6.7 and 6.8, respectively, as well as the imaginary frequency of the TS. Several low frequencies (below 300 $cm^{-1}$) in addition to the imaginary frequency were calculated for the hydrogen-abstraction TS. Of these, three were identified as internal rotations (or torsional vibrations) by visualization of the normal modes. These harmonic modes correspond most closely to the three new internal rotors created in the TS ($XCOH^{\cdots}ONO_2$, $XCO^{\cdots}HNO_3$ and $XCOHO^{\cdots}NO_2$), where the common axes for internal rotation are the ones linking the reactants, products, and one along the N-O bond with the oxygen atom abstracting the hydrogen. These were the axes considered in the calculation of the reduced moments of inertia. These harmonic modes were treated as free rotors in the calculation of the internal-rotation partition function of the TS ($Q_{IR}^{TS}$).[32,33] A similar procedure has been used in earlier related studies.[5,34]

The harmonic contributions of these low frequencies were eliminated from the vibrational partition function in order to correct the total partition function of the TS ($Q_{corr}^{TS}$):

$$Q_{corr}^{TS} = \frac{Q^{TS}\, Q_{IR}^{TS}}{\prod Q_{v=i}} \tag{6.2}$$

For $CH_3CHO$ and its TS, the internal rotation around the C-C single bond was also considered and treated as a free rotor.

TST direct rate constants ($k_D$) at 298 K for the reactions of $CH_3CHO$ and HCHO with $NO_3$ radicals, calculated at different levels of theory, are given in Tables 6.9 and 6.10, respectively. Some experimental results have been included for comparison. The tunneling corrections ($\kappa$) and $\Delta s_{1/2}$ are also reported.

**Table 6.7.** Total partition functions (Q) of the reactants and the TS, and imaginary frequency ($\nu^{\neq}$ in $cm^{-1}$) of the TS of the $NO_3$ hydrogen-abstraction reaction from XCHO (X = F, Cl, H, $CH_3$), calculated at the MP2(FC)/6-311G(d,p) level of theory.

| System | **FCHO + $NO_3$** | **ClCHO + $NO_3$** | **HCHO + $NO_3$** | **$CH_3CHO$ + $NO_3$** |
|---|---|---|---|---|
| $Q^{NO_3\,(D_{3h})}$ | $1.70737\cdot10^{11}$ | $1.70737\cdot10^{11}$ | $1.70737\cdot10^{11}$ | $1.70737\cdot10^{11}$ |
| $Q^{XCHO}$ | $1.13573\cdot10^{11}$ | $3.90682\cdot10^{11}$ | $4.61479\cdot10^{9}$ | $2.97963\cdot10^{11}$ [(a)] |
| $Q^{TS}$ | $3.90874\cdot10^{15}$ | $1.44419\cdot10^{16}$ | $7.39244\cdot10^{14}$ | $1.53333\cdot10^{16}$ |
| $\prod Q_{v=i}$ [(f)] | 28.649 [(b)] | 41.307 [(c)] | 17.383 [(d)] | 90.815 [(e)] |
| $Q_{IR}^{TS}$ [(g)] | $4.78689\cdot10^{4}$ | $8.51824\cdot10^{4}$ | $1.55481\cdot10^{4}$ | $1.64320\cdot10^{5}$ |
| $Q_{corr}^{TS}$ [(h)] | $6.53102\cdot10^{18}$ | $2.97821\cdot10^{19}$ | $6.61219\cdot10^{17}$ | $2.77441\cdot10^{19}$ |
| $\nu^{\neq}$ | 2703 | 2335 | 1395 | 998 |

[(a)] $Q_{corr}^{CH_3CHO} = 5.39632\cdot10^{11}$; [(b)] i=1, 3, 4; [(c)] i=1, 3, 4; [(d)] i=1, 2, 4; [(e)] i=1, 2, 4, 6;
[(f)] Vibrational components that were eliminated from the calculation of $Q_{corr}^{TS}$; [(g)] Total internal-rotational partition function of the TS; [(h)] Corrected total partition function of the TS

**Table 6.8.** Total partition functions (Q) of the reactants and the TS, and imaginary frequency ($\nu^{\neq}$ in $cm^{-1}$) of the TS of the $NO_3$ hydrogen-abstraction reaction from XCHO (X = F, Cl, H, $CH_3$), calculated at the BH&HLYP/6-311G(d,p) level of theory.[(a)]

| System | **FCHO + $NO_3$** | **ClCHO + $NO_3$** | **HCHO + $NO_3$** | **$CH_3CHO$ + $NO_3$** |
|---|---|---|---|---|
| $Q^{NO_3\,(C_{2v})}$ | $5.50530\cdot10^{11}$ | $5.50530\cdot10^{11}$ | $5.50530\cdot10^{11}$ | $5.50530\cdot10^{11}$ |
| $Q^{XCHO}$ | $1.08003\cdot10^{11}$ | $3.79813\cdot10^{11}$ | $4.42745\cdot10^{9}$ | $2.79523\cdot10^{11}$ [(b)] |
| $Q^{TS}$ | $5.34208\cdot10^{15}$ | $1.82529\cdot10^{16}$ | $1.09900\cdot10^{15}$ | $8.36021\cdot10^{16}$ |
| $\prod Q_{v=i}$ | 33.585 [(c)] | 48.383 [(d)] | 23.921 [(e)] | 393.66 [(f)] |
| $Q_{IR}^{TS}$ | $4.68184\cdot10^{4}$ | $8.46634\cdot10^{4}$ | $1.38936\cdot10^{4}$ | $1.66813\cdot10^{5}$ |
| $Q_{corr}^{TS}$ | $7.44708\cdot10^{18}$ | $3.19401\cdot10^{19}$ | $6.38324\cdot10^{17}$ | $3.54265\cdot10^{19}$ |
| $\nu^{\neq}$ | 1983 | 1503 | 239 | 141 |

[(a)] See footnotes of Table 6.7 for more details; [(b)] $Q_{corr}^{CH_3CHO} = 5.10774\cdot10^{11}$;
[(c)] i=1, 3, 4; [(d)] i=1, 3, 4; [(e)] i=1, 2, 4; [(f)] i=1, 2, 4, 6

In both cases the CCSD(T)//BH&HLYP* calculation gives the best rate constants, $1.11 \cdot 10^6$ for $CH_3CHO + NO_3$ and $2.09 \cdot 10^5$ for $HCHO + NO_3$, in very good agreement with experimental values of $1.26\text{-}1.69 \cdot 10^6$ for $CH_3CHO + NO_3$ and $1.95\text{-}3.79 \cdot 10^5$ for $HCHO + NO_3$. Rate constants at other levels of calculation are not able to reproduce the order of the experimental values for both reactions. From this, it is concluded that CCSD(T)//BH&HLYP* is the best method for predicting kinetic parameters in these systems.

**Table 6.9.** Rate constants (in L/mol·s) and tunneling parameters for the $NO_3$ hydrogen-abstraction reaction from $CH_3CHO$, calculated at different levels of theory using the 6-311G(d,p) basis set, and considering a direct mechanism, at 298.15 K.

| Level of Calculation: | $\kappa_D$ [(a)] | $\Delta s_{½}$ [(b)] | $k_D$ |
|---|---|---|---|
| PMP2 | 3.33 | | $3.82 \cdot 10^{-10}$ |
| CCSD(T)//MP2(FC) | 2.81 | 0.70 | $4.45 \cdot 10^5$ |
| BH&HLYP | - | | $8.69 \cdot 10^8$ |
| CCSD(T)//BH&HLYP | 1.02 | | $9.51 \cdot 10^7$ |
| BH&HLYP + BSSE(BH&H) | 1.02 | | $4.95 \cdot 10^7$ |
| CCSD(T)//BH&HLYP + BSSE(BH&H) | 1.02 | | $5.31 \cdot 10^6$ |
| CCSD(T)//BH&HLYP + BSSE(CC) | 1.02 | | $4.10 \cdot 10^5$ |
| CCSD(T)//BH&HLYP* | 1.02 | 3.57 | $1.11 \cdot 10^6$ |
| Experiment | | | $1.58 \cdot 10^6$ [(c)] |
| | | | $1.64 \cdot 10^6$ [(d)] |
| | | | $1.44 \cdot 10^6$ [(e)] |
| | | | $1.67 \cdot 10^6$ [(f)] |
| | | | $1.69 \cdot 10^6$ [(g)] |
| | | | $1.26 \cdot 10^6$ [(h)] |

[(a)] Tunneling correction; [(b)] Full width of the barrier at half its height, in Å;
[(c)] Ref. 21a(2001); [(d)] Ref. 3a(1999), 3b(1997); [(e)] Ref. 3c(1997); [(f)] Ref. 20a(1991); [(g)] Ref. 21b(1989); [(h)] Ref. 13a(1986)

**Table 6.10.** Rate constants (in L/mol·s) and tunneling parameters for the $NO_3$ hydrogen-abstraction reaction from HCHO, calculated at different levels of theory using the 6-311G(d,p) basis set, for both the direct and complex mechanisms at 298.15 K.

| | **Direct Mechanism** | | | **Complex Mechanism** | | |
|---|---|---|---|---|---|---|
| Level of Calculation: | $\kappa_D$[(a)] | $\Delta s_{½}$[(b)] | $k_D$ | $\kappa$[(a)] | $\Delta s_{½}$[(b)] | $k_{eff}$ |
| PMP2 | 23.16 | | $2.39\cdot10^{-10}$ | 11.97 | | $1.24\cdot10^{-10}$ |
| CCSD(T)//MP2(FC) | 8.96 | 0.51 | $9.66\cdot10^{4}$ | 11.08 | 0.59 | $1.19\cdot10^{5}$ |
| BH&HLYP | 1.05 | | $4.78\cdot10^{8}$ | 1.06 | | $4.81\cdot10^{8}$ |
| CCSD(T)//BH&HLYP | 1.06 | | $1.78\cdot10^{7}$ | 1.06 | | $1.78\cdot10^{7}$ |
| BH&HLYP + BSSE(BH&H) | 1.06 | | $2.86\cdot10^{7}$ | 1.06 | | $2.86\cdot10^{7}$ |
| CCSD(T)//BH&HLYP + BSSE(BH&H) | 1.06 | | $1.06\cdot10^{6}$ | 1.06 | | $1.06\cdot10^{6}$ |
| CCSD(T)//BH&HLYP* | 1.06 | 2.47 | $2.09\cdot10^{5}$ | 1.06 | 2.22 | $2.08\cdot10^{5}$ |
| Experiment | | | $3.49\cdot10^{5}$ [(c)]<br>$3.25\cdot10^{5}$ [(d)]<br>$3.79\cdot10^{5}$ [(e)]<br>$1.95\cdot10^{5}$ [(f)] | | | |

[(a)] Tunneling correction; [(b)] Full width of the barrier at half its height, in Å;
[(c)] Ref. 3a(1999), 3b, 3c (1997), 20a(1991); [(d)] Ref. 20b(1988); [(e)] Ref. 20c(1985); [(f)] Ref. 20d(1984)

### *6.3.2.1. **Elementary or complex reactions?***

The significance of considering the complex character of the kinetics of a radical-molecule reaction was one of the main conclusions of a recent work.[5a] Later it was shown that even for reactions with less stable reactant complexes and higher activation energies (FCHO + OH and ClCHO + OH),[5b] a complex mechanism should also be considered. Furthermore, it was shown that for these two reactions, the percentage difference between the elementary (direct) and complex (effective) rate constants was smaller than the

difference found for the HCHO + OH reaction, in which a smaller activation energy was found. It was rationalized that the bigger the effective energy barrier for radical-molecule reactions, and the smaller the stabilization energy of the reactant complex, the more closely its behaviour resembles an elementary reaction.

Intuitively, for the $NO_3$ reactions higher activation energies and less stable reactant complexes are expected. Hence, a smaller percentage of difference between the elementary and complex rate constants in comparison with the analogous OH reactions is also expected. In other words, the kinetic behaviour of the $NO_3$ reactions should resemble more closely an elementary reaction. Whether these reactions should be assumed elementary or whether the formation of the reactant complex must be considered, will be discussed in this section.

For the simplest system, the HCHO + $NO_3$ reaction, two possible mechanisms were considered: a direct mechanism, in which the hydrogen-abstraction takes place in an elementary step, and a two-step mechanism that involves a fast pre-equilibrium between the reactants and the reactant complex, followed by the irreversible hydrogen-abstraction that takes place in the reactant complex to form the products (product complex):

Step 1: $HCHO + NO_3 \leftrightarrows [HCHO^{\cdots}NO_3]$

Step 2: $[HCHO^{\cdots}NO_3] \rightarrow [HCO^{\cdots}HNO_3] \rightarrow HCO + HNO_3$

As shown before (Chapter 4) the overall rate constant for the complex mechanism ($k_{eff}$) can be calculated by:

$$k_{eff} = \kappa \frac{k_B T}{h} \frac{Q^{TS}}{Q^{React}} \exp\left(-\frac{\left(E^{TS} - E^{React}\right)}{RT}\right) \tag{6.3}$$

The geometry of the reactant and product complexes of the HCHO + $NO_3$ reaction are shown in Figure 6.1, where some geometrical parameters have been indicated. These structures have been determined by dipole-dipole interactions.

(a) $HCHO^{\cdots}NO_3$

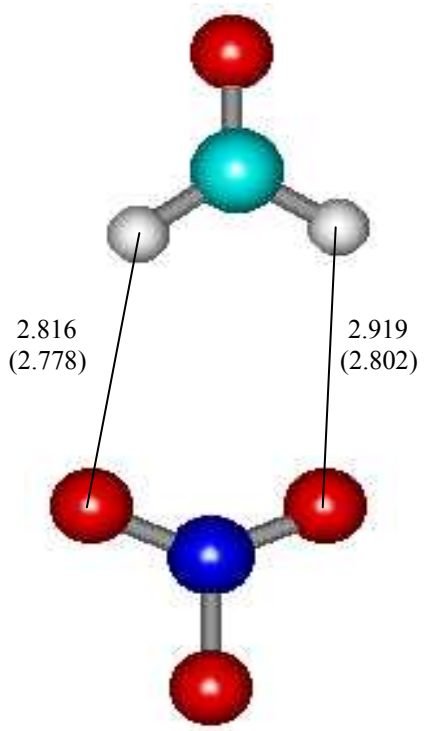


(b) $HCO^{\cdots}HNO_3$

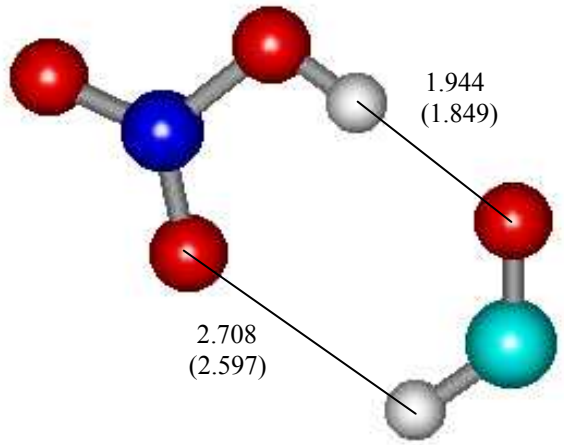


**Figure 6.1.** Optimized structures of the (a) reactant and (b) product complexes in the HCHO + $NO_3$ hydrogen-abstraction reaction, as obtained at the MP2(FC) (BH&HLYP) level with the 6-311G(d,p) basis set.
(Bond distances are given in Å)

The stabilization energy of the reactant complex ($E_{a\ (-1)}$) and the activation barrier of the second step of the complex mechanism ($E_{a\ (2)}$) at 0 K, are given in Table 6.6. At the CCSD(T)//MP2(FC) level the reactant complex is calculated to be 10.7 kJ/mol lower in energy than the isolated reactants. At this level, but using a slightly larger basis set: 6-311++G(d,p), the stabilization energy of the reactant complex for the HCHO + OH reaction is calculated to be 13.6 kJ/mol. The new complex is less stable, as expected. At the CCSD(T)//BH&HLYP level this energy is 6.7 kJ/mol. The actual reactant complex stabilization energy is expected to be between these two values (6.7 and 10.7 kJ/mol).

Rate constants calculated for the direct and complex mechanisms are reported in Table 6.10. At the CCSD(T)//MP2 level the difference is small. The percentage by which these two rate constants differ, calculated by:

$$\left(\frac{k_{eff} - k_D}{k_{eff}}\right) \cdot 100\% \qquad (6.4)$$

is 18.8%. For the OH hydrogen-abstraction reaction from the same series of aldehydes, this percentage difference is 71.3 for the FCHO reaction, the one with the highest activation energy and the least stable reactant complex (see Chapter 5). For the other calculations the difference between rate constants for the mechanisms considered is negligible. Hence, the assumption of an elementary mechanism for the $NO_3$ hydrogen-abstraction reaction from these aldehydes is valid.

### *6.3.3.* ***Results and discussions on the $NO_3$ hydrogen-abstraction reactions***

The optimized geometries of the TSs of these reactions are shown in Fig. 6.2, where relevant geometrical parameters have been indicated for the MP2 and BH&HLYP optimizations. The overall shape of these molecular systems did not change significantly at these two levels. The reaction profiles at the CCSD(T)/BH&HLYP* level of calculation are shown in Fig. 6.3.

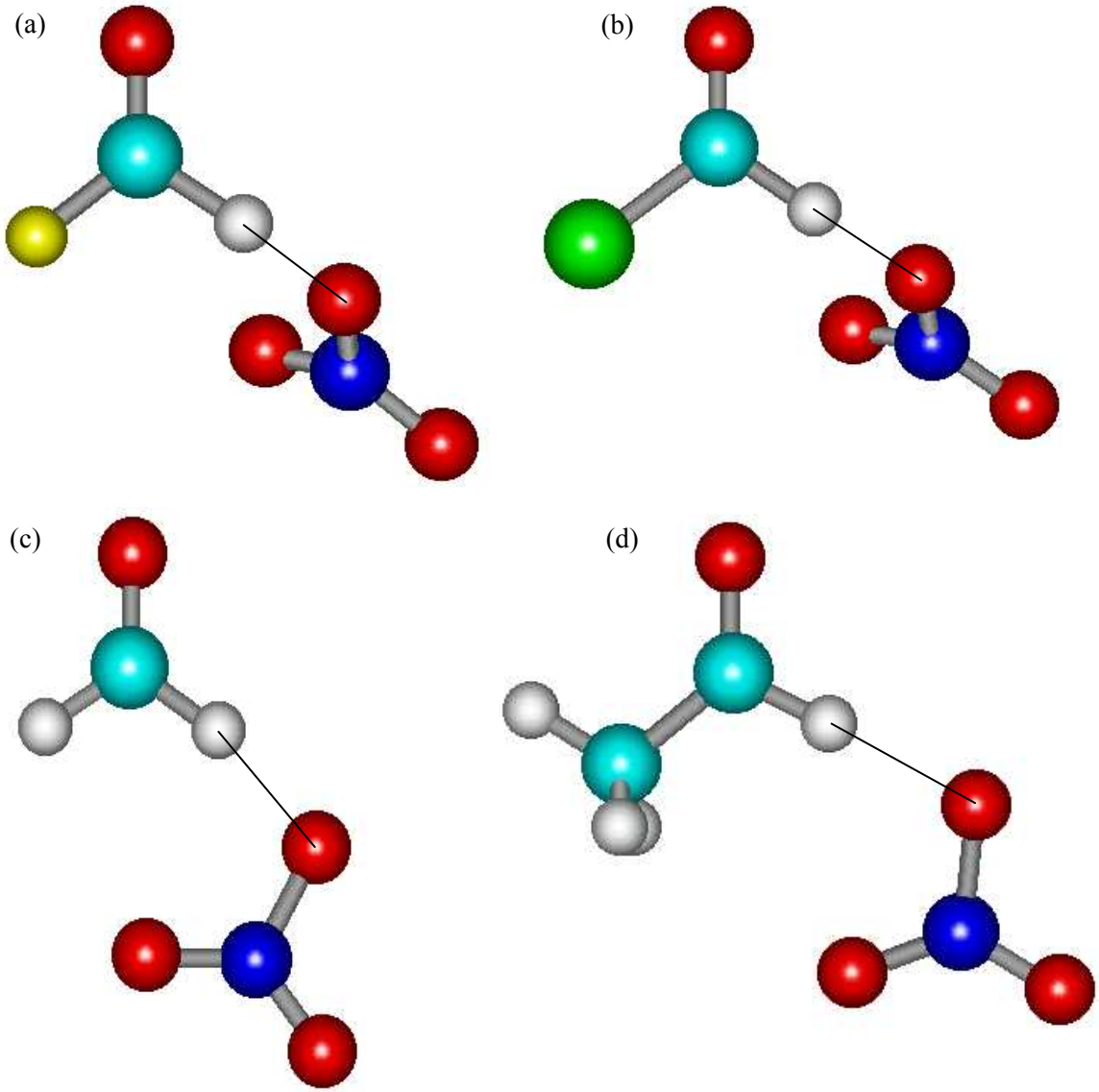


| **X**(O)C···H···$ONO_2$ | **MP2(FC)/6-311G(d,p)** | | | **BH&HLYP/6-311G(d,p)** | | |
|---|---|---|---|---|---|---|
| **X** | d(C,H) | d(H,O) | ∠(C,H,O) | d(C,H) | d(H,O) | ∠(C,H,O) |
| F | 1.195 | 1.359 | 174.3 | 1.240 | 1.287 | 174.9 |
| Cl | 1.178 | 1.424 | 176.7 | 1.200 | 1.372 | 177.9 |
| H | 1.164 | 1.563 | 168.9 | 1.146 | 1.617 | 165.3 |
| $CH_3$ | 1.160 | 1.595 | 175.9 | 1.132 | 1.735 | 179.3 |

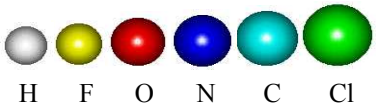


**Figure 6.2.** Structure of the transition states of the hydrogen-abstraction reactions studied and some relevant geometrical parameters. (a) FCHO + $NO_3$, (b) ClCHO + $NO_3$, (c) HCHO + $NO_3$, (d) $CH_3CHO$ + $NO_3$.
(Bond distances are given in Å and angles in degrees)

$$XCHO + NO_3 \longrightarrow XCO + HNO_3 \quad (X = F, Cl, H, CH_3)$$

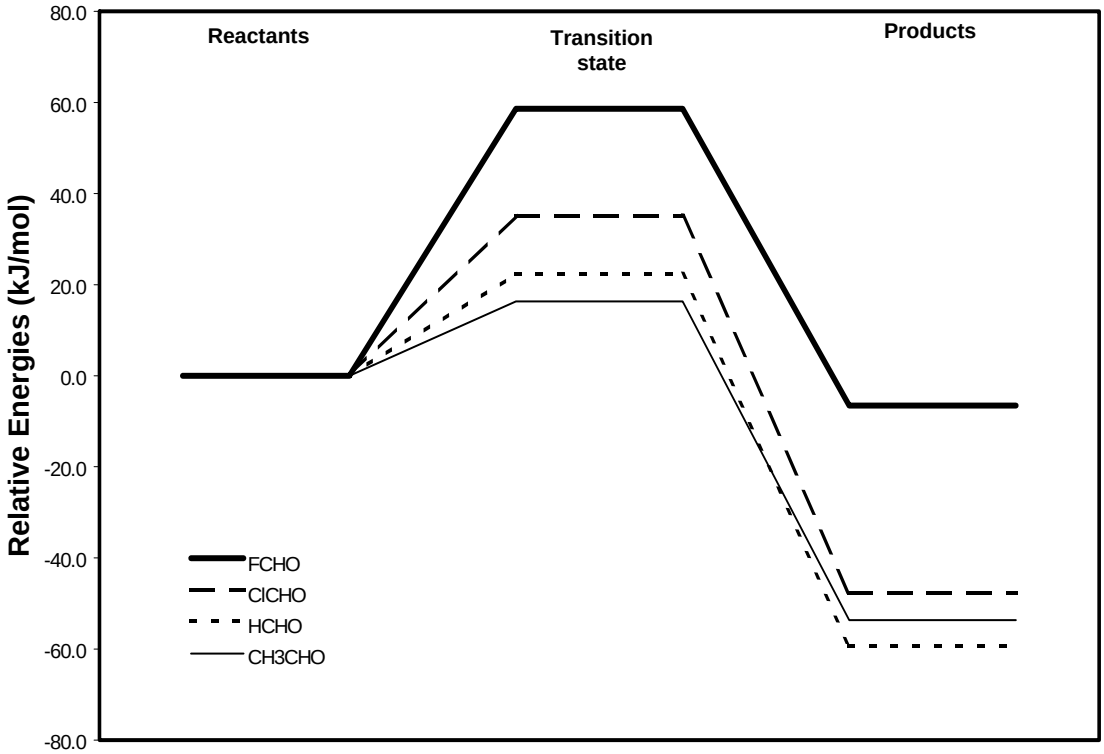


**Figure 6.3.** Schematic reaction profile for the XCHO + $NO_3$ (X = F, Cl, H, $CH_3$) hydrogen-Abstraction reactions using the calculated CCSD(T)/6-311G(d,p)//BH&HLYP/6-311G(d,p) energy values, including the BH&HLYP/6-311G(d,p) zero-point energy corrections.

*Note:* For the CCSD(T) calculation on the $NO_3$ radical the MP2(FC)-$D_{3h}$ geometry was employed.

The symmetry of the TS calculated for the $NO_3$ reaction with HCHO and $CH_3CHO$ is $^2A'$, ($C_s$ point group) implying that the unpaired electron is in the plane where the $NO_3$ attack takes place. $^2A'$ is also the symmetry of the XCO radical generated. This corresponds to the TS structures obtained for the OH reactions. However, for the FCHO and ClCHO hydrogen-abstraction reaction, the TSs possess $C_1$ symmetry. The oxygen atoms of the $NO_3$ radical avoid spatial interaction with the electronic cloud of the halogen atom of these aldehydes, and the best way of achieving this, without creating new destabilizing interactions, is by breaking the plane of symmetry. Hydrogen bonding interactions stabilize these structures. For HCHO and $CH_3CHO$ the distance from the closest oxygen atom (of the two not directly implied in the abstraction process) of $NO_3$ to the aldehyde is 2.605 and 2.931 Å, respectively. For FCHO and ClCHO these distances are 3.172 and 3.611 Å, respectively. The larger the halogen atom the greater this interatomic distance. The structure of the TS of the $CH_3CHO$ reaction reported in the work by D'Anna andcoworkers,[21a] calculated at the MP2/cc-pVDZ level of theory, agrees to within 0.01 Å with the MP2 results reported here.

In the series of substituents, F, Cl, H and $CH_3$, the TS is achieved earlier. Thus, the calculated C···H distances decrease in this order from 1.195 Å (FCHO) to 1.160 ($CH_3CHO$) at the MP2 level and from 1.240 to 1.132 Å at the BH&HLYP level; in a similar way the H···O distance increases. Furthermore, a larger activation energy has to be overcome. This trend is consistent with the decreasing electron-donating effect of these substituents that is also the cause of the decreasing reactivity of these aldehydes towards the $NO_3$ hydrogen-abstraction reaction. Similar results were discussed for the analogous OH reactions in Chapter 5.[5b]

Constant oscillations between energy related structures during the optimization of the TS, and the reactant and product complexes (in the case of the HCHO + $NO_3$ reaction) are difficult to overcome. These oscillations basically involve the stretching and enlargement of the NO bonds in the $NO_3$ radical, and may be related to the "symmetry dilemma" for this radical, discussed above.

Frequency calculations at MP2 level lead to imaginary frequencies of the TS where the transfer of the hydrogen atom between the carbon and oxygen atoms is easy to visualize for the four reactions. In a similar way the large amplitude vibrations were assigned to internal rotations and the axes were identified, as explained before in Section 6.3.2. At the BH&HLYP level the situation is quite different. Only the TS of the FCHO and ClCHO reactions showed imaginary frequencies like the one described above. However, for the HCHO and $CH_3CHO$ reactions this vibrational mode exhibits features of an addition-elimination reaction. IRC calculations proved that the optimized structures are the TSs of the aldehydic hydrogen-abstraction reactions, and moreover, made possible the establishment of a relationship between the TS of the HCHO reaction and the corresponding reactant and product complexes referred to in Section 6.3.2.1. An analogous situation was encountered while studying the HCHO + OH hydrogen-abstraction reaction at the B3LYP level, but at the BH&HLYP level this is not the case. This problem may be an artefact of the method.

In the series of substituents, F, Cl, H, $CH_3$, the imaginary frequency of the TS ($\nu^{\neq}$) decreases at both levels of theory, and thus the curvature of the calculated barrier is reduced as well; $\Delta s_{½}$ increases in the same order. In this series of aldehydes $\kappa$ decreases in agreement with the fact that activation energies and imaginary frequencies decrease. At the MP2 and BH&HLYP levels of theory barriers are predicted to reduce in height and curvature on going from FCHO to $CH_3CHO$. This is also the case for the OH hydrogen-abstraction reactions.

Barriers calculated using BH&HLYP geometries are predicted to be smaller and wider than those calculated with MP2 structures, as expected. Tunneling corrections for BH&HLYP geometries are significantly smaller than the values calculated with MP2 structures, since barriers and imaginary frequencies are also smaller.

Cartesian coordinates of the TS, reactant and product complexes at MP2 and BH&HLYP levels are available,[35] as well as the calculated total energies (PMP2, CCSD(T)//MP2, BH&HLYP and CCSD(T)// BH&HLYP), zero-point and thermal (at 298.15 K)

vibrational energy corrections (calculated at MP2 and BH&HLYP levels) of the species involved in the reaction of $NO_3$ with the aldehydes, and the BSSE calculated for the TS for these reactions.

The remaining parameters were calculated at the CCSD(T)//BH&HLYP* level, at which the experimental kinetic parameters and reaction enthalpies are reproduced. The predicted values of rate constant and activation energy for the $NO_3$ hydrogen-abstraction reaction from FCHO and ClCHO, at 298K, are: 60.2 kJ/mol and 10.30 L/mol·s for FCHO, and 37.0 kJ/mol and $9.01 \cdot 10^8$ L/mol·s for ClCHO. Reaction enthalpies are calculated to be -6.4 (FCHO) and -47.1 kJ/mol (ClCHO). These values, as well as activation energies and reaction enthalpies at 0 K and tunneling parameters calculated at various levels of theory are shown in Tables 6.11 and 6.12. The calculated partition functions and imaginary frequency of the TS at MP2 and BH&HLYP levels are given in Tables 6.7 and 6.8, respectively.

In order to obtain the CCSD(T) energy differences reported in Tables 6.5, 6.6 and 6.11, vibrational corrections at the level at which the geometries were optimized, MP2 or BH&HLYP, are used. For these reactions spin contamination at the TS is small; the highest expectation value of $S^2$ is 0.806 for the FCHO reaction at the MP2 level. Spin contamination is completely eliminated by projection at MP2 and BH&HLYP levels, hence CCSD(T) calculations may be considered reliable in this sense.

For the HCHO and $CH_3CHO$ reactions with $NO_3$ radicals with geometries calculated at the BH&HLYP level, tunneling corrections are almost negligible (1.06 and 1.02, respectively). Hence, an Arrhenius behaviour is expected for these reactions at temperatures above $T^*$, the characteristic tunneling temperature below which tunneling is significant. $T^*$ is equal to $hc\nu^{\neq}/(2\pi k_B)$; for the HCHO and $CH_3CHO$ reactions, T* is 55 and 32 K, respectively. Hence, classical Arrhenius parameters for these reactions for temperatures above $T^*$ may be calculated from:

$$A = \frac{k_B T}{h} \frac{Q^{TS}}{Q^{React}} \tag{6.5}$$

**Table 6.11.** Activation energy ($E_a$) and reaction enthalpy ($\Delta H$), in kJ/mol, including zero-point (ZPE) or thermal vibrational corrections at 298.15 K (TCE), for the $NO_3$ hydrogen-abstraction reaction from XCHO (X = F, Cl, H) at different levels of theory.

| Basis set: 6-311G(d,p) | $E_a^{(ZPE)}$ | $E_a^{(TCE)}$ | $\Delta H^{(ZPE)}$ | $\Delta H^{(TCE)}$ |
|---|---|---|---|---|
| **FCHO + $NO_3$** | | | | |
| PMP2 | 147.8 | 149.6 | 15.9 | 16.8 |
| CCSD(T)//MP2(FC) | 74.4 | 76.3 | -28.2 | -27.3 |
| BH&HLYP | 49.3 | 51.0 | -13.4 | -13.3 |
| CCSD(T)//BH&HLYP | 47.6 | 49.2 | -17.5 | -17.4 |
| BH&HLYP + BSSE(BH&H) | 58.5 | 60.1 | | |
| CCSD(T)//BH&HLYP + BSSE(BH&H) | 56.7 | 58.4 | | |
| CCSD(T)//BH&HLYP* | 58.6 | 60.2 | -6.5 | -6.4 |
| **ClCHO + $NO_3$** | | | | |
| PMP2 | 131.5 | 133.7 | -25.1 | -23.9 |
| CCSD(T)//MP2(FC) | 52.5 | 54.7 | -68.7 | -67.5 |
| BH&HLYP | 28.1 | 30.0 | -55.5 | -54.8 |
| CCSD(T)//BH&HLYP | 24.2 | 26.0 | -58.8 | -58.2 |
| BH&HLYP + BSSE(BH&H) | 37.3 | 39.1 | | |
| CCSD(T)//BH&HLYP + BSSE(BH&H) | 33.3 | 35.2 | | |
| CCSD(T)//BH&HLYP* | 35.2 | 37.0 | -47.8 | -47.1 |

**Table 6.12.** Rate constants (in L/mol·s) and tunneling parameters for the $NO_3$ hydrogen-abstraction reaction from FCHO and ClCHO, calculated at different levels of theory using the 6-311G(d,p) basis set, and considering a direct mechanism, at 298.15 K.

| | **FCHO + $NO_3$** | | | **ClCHO + $NO_3$** | | |
|---|---|---|---|---|---|---|
| Level of Calculation: | $\kappa_D$ | $\Delta s_{½}$ | $k_D$ | $\kappa_D$ | $\Delta s_{½}$ | $k_D$ |
| PMP2 | $4.53\cdot10^{7}$ | | $1.23\cdot10^{-9}$ | $1.11\cdot10^{6}$ | | $2.80\cdot10^{-8}$ |
| CCSD(T)//MP2(FC) | $8.05\cdot10^{4}$ | 0.41 | 15.55 | $1.34\cdot10^{3}$ | 0.39 | $2.36\cdot10^{3}$ |
| BH&HLYP | 162.25 | | $2.85\cdot10^{2}$ | 11.19 | | $1.25\cdot10^{5}$ |
| CCSD(T)//BH&HLYP | 152.76 | | $5.49\cdot10^{2}$ | 9.66 | | $5.34\cdot10^{5}$ |
| BH&HLYP + BSSE(BH&H) | 273.18 | | 11.92 | 14.76 | | $4.11\cdot10^{3}$ |
| CCSD(T)//BH&HLYP + BSSE(BH&H) | 260.34 | | 23.42 | 13.19 | | $1.81\cdot10^{4}$ |
| CCSD(T)//BH&HLYP* | 244.78 | 0.50 | 10.30 | 13.95 | 0.49 | $9.01\cdot10^{3}$ |

For $CH_3CHO$ + $NO_3$ the pre-exponential factor (in units of L/mol·s) is calculated to be $7.83\cdot10^{8}$, in very good agreement with the experimental value ($8.43$ - $8.67\cdot10^{8}$, see Table 6.3). For the HCHO + $NO_3$ reaction the Arrhenius parameter is predicted to be $1.63\cdot10^{9}$, basically twice the A value for the $CH_3CHO$ reaction, as expected since in HCHO there are two equivalent sites of attack. The suggested value[3a] $1.20\cdot10^{9}$ is in agreement with this calculation.

For the FCHO and ClCHO reactions tunneling is significant. The calculated characteristic temperature ($T^*$) is 454 and 344 K, respectively. Calculations of Arrhenius parameters using the above expression and ignoring tunneling quantum effects would be erroneous. If the value of κ is included in the above expression, A for the FCHO and ClCHO

reactions would be $1.90 \cdot 10^{11}$ and $1.32 \cdot 10^{10}$, respectively. Although this is not the most appropriate way of estimating the quantum Arrhenius parameter, these values could be used as a reference when better determinations are made.

## 6.4. Conclusions

The $NO_3$ hydrogen-abstraction reaction from a series of aldehydes (XCHO: X = F, Cl, H, $CH_3$) has been studied by means of *ab initio* calculations. Optimizations at the MP2 and BH&HLYP levels followed by CCSD(T) single point calculations were performed using the 6-311G(d,p) basis set. Neither CCSD(T)//MP2 nor CCSD(T)//BH&HLYP calculations were successful in reproducing the kinetic and thermochemical data available for such reactions. Hence several corrections were considered to improve upon the CCSD(T)//BH&HLYP results, which were the closest to experiment. The use of the MP2-$D_{3h}$ geometry of the $NO_3$ radical (for which a lot of controversial results regarding its ground state symmetry have been published) in the CCSD(T) calculation reproduced the only 6 parameters for which experimental results exist: rate constants and reaction enthalpies for the $CH_3CHO$ and HCHO reactions, as well as the activation energy and Arrhenius pre-exponential factor for the $CH_3CHO$ reaction with $NO_3$ radicals. At this level of theory the remaining parameters were then predicted theoretically for the first time, since no previous theoretical studies have been reported for the reactions between aldehydes and $NO_3$ radicals.

It was shown that these reactions can be considered elementary. The consideration of a reactant complex as in previous studies (Chapters 4 and 5)[5] does not affect the calculated kinetic results at the chosen level of theory. These results complement a series of studies regarding radical-molecule reactions and prove that even though for some reactions with low or negative activation energies the formation of the reactant complex needs to be considered, another extreme case, such as the $NO_3$ reactions studied, can be found for which a one-step mechanism is a sufficient approximation for kinetic determinations.[5b]

## 6.5. References


1. Finlayson-Pitts, B.J.; Pitts, J.N. *Atmospheric Chemistry: Fundamentals and Experimental Techniques*, Wiley Interscience, New York, 1986.

2. Seinfeld, J.H.; Pandis, S.N. *Atmospheric Chemistry and Physics: From Air Pollution to Climate Change*, Wiley Interscience, New York, 1998.

3. (a) Atkinson, R.; Baulch, D.L.; Cox, R.A.; Hampson, R.F. Jr.; Kerr, J.A.; Rossi, M.J.; Troe, J. *J. Phys. Chem. Ref. Data* **1999**, *28*, 191. (b) Atkinson, R.; Baulch, D.L.; Cox, R.A.; Hampson, R.F., Jr.; Kerr, J.A.; Rossi, M.J.; Troe, J. *J. Phys. Chem. Ref. Data* **1997**, *26*, 521. (c) DeMore, W.B.; Sander, S.P.; Golden, D.M.; Hampson, R.F.; Kurylo, M.J.; Howard, C.J.; Ravishankara, A.R.; Kolb, C.E.; Molina, M.J. *JPL Publication* 97-4 **1997**. (d) Taylor, P.H.; Rahman, M.S.; Arif, M.; Dellinger, B.; Marshall, P. *Symp. Int. Combust. Proc.* **1996**, *26*, 497. (e) Wallington, T.J.; Hurley, M.D. *Environ. Sci. Technol.* **1993**, *27*, 1448. (f) Francisco, J.S. *J. Chem. Phys.* **1992**, *96*, 7597. (g) Libuda, H.G.; Zabel, F.; Fink, E.H.; Becker, K.H. *J. Phys. Chem.* **1990**, *94*, 5860, and references therein.

4. The NIST Chemical Kinetics Database, NIST Standard Reference Database, U.S. Dept. of Commerce, Technology Administration, National Institute of Standards and Technology: Gaithersburg, MD, 17-2Q98.

5. (a) Alvarez-Idaboy, J.R.; Mora-Diez, N.; Boyd, R.J.; Vivier-Bunge, A. *J. Am. Chem. Soc.*, **2001**, *123*, 2018. (b) Mora-Diez, N.; Alvarez-Idaboy, J.R.; Boyd, R.J. *J. Phys. Chem.*, **2001**, in press.

6. (a) Wallington, T.J.; Hurley, M.D.; Ball, J.C.; Kaiser, E.W. *Environ. Sci. Technol.* **1992**, *26*, 1318. (b) Hasson, A.S.; Moore, C.M.; Smith, I.W.M. *Int. J. Chem. Kinet.* **1998**, *30*, 541. (c) Sanhueza, E.C.; Heicklen, J. *J. Phys. Chem.* **1975**, *79*, 7. (d) Gay, B.W.; Hanst, P.L.; Bufalini, J.J.; Noonan, R.C. *Environ. Sci. Technol.* **1976**, *10*, 58. (e) Niki, H.; Maker, P.D.; Savage, C.M.; Breitenbach, L.P. *Int. J. Chem. Kinet.* **1980**, *12*, 1001. (f) Niki, H.; Maker, P.D.; Savage, C.M.; Breitenbach, L.P.; Martinez, R.I.; Herron J.T. *J. Phys. Chem.* **1982**, *86*, 1858. (g) Tuazon, E.C.; Atkinson R.; Aschmann, S.M.; Goodman, M.A.; Winer, A.M. *Int. J. Chem. Kinet.* **1988**, *20*, 241. (h) Fantechi, G.; Jensen, N.R.; Saastad, O.; Hjorth, J.; Peeters, J. *J. Atmos. Chem.* **1998**, *31*, 247.

7. (a) Eyring, H. *J. Chem. Phys.* **1935**, *3*, 107. (b) Evans, M.G., Polanyi, M. *Trans. Faraday Soc.* **1935**, *31*, 875.

8. (a) Eckart, C. *Phys. Rev.* **1930**, *35*, 1303. (b) Shin, H. *J. Chem. Phys.* **1963**, *39*, 2934.

9. Noxon, J.F.; Norton, R.B.; Henderson, W.R. *J. Geophys. Res.* **1978**, *5*, 675.

10. (a) Platt, U.; Perner, D.; Winer, A.M.; Harris, G.W.; Pitts, N.J. *Geophys. Res. Lett.* **1980**, *7*, 89. (b) Noxon, J.F.; Norton, R.B.; Marovich, E. *Geophys. Res. Lett.* **1980**, *7*, 125.

11. Atkinson, R. *Atmos. Environ.* **2000**, *34*, 2063.

12. (a) Calvert, J.G.; Stockwell. W.R. *Environ. Sci. Technol.* **1983**, *17*, 428A. (b) Atkinson, R.; Plum, C.N.; Carter, W.P.L.; Winer, A.M.; Pitts, J.N., Jr. *J. Phys. Chem.* **1984**, *88*, 2361. (c) Seinfeld, J.H. *Science* **1989**, *243*, 745. (d) Schwartz, S.E. *ibid.*, 753. (e) McElroy, M.B.; Salawitch, R.J. *ibid.*, 763.

13. (a) Louw, R.; van Harm, J.; Nieboer, H. *J. Air Pollut. Contr. Ass.* **1973**, *23*, 716. (b) Cantrell, C.A.; Davidson, J.A.; Busarow, K.L.; Calvert, J.G. *J. Geophys. Res.* **1986**, *91*, 5347. (c) Miller, C.E.; Francisco, J.S. *J. Phys. Chem.* **2001**, *105*, 750.

14. Bandow, H.; Okuda, M.; Akimoto, H. *J. Phys. Chem.* **1980**, *84*, 3604.

15. Wayne, R.P.; Barnes, I.; Biggs, P.; Burrows, J.P.; Canosa-Mas, C.E.; Hjorth, J.; Le Bras, G., Moortgat, G.K.; Perner, D.; Poulet, G.; Restelli, G.; Sidebottom, H. *Atmos. Environ.* **1991**, *25A*, 1.

16. (a) D'Anna, B.; Nielsen, C.J. *J. Chem. Soc. Faraday Trans.* **1997**, *93*, 3479. (b) Monks, P.S.; Stief, L.J.; Krauss, M.; Kuo, S.C.; Zhang, Z.; Klemm, R.B. *J. Phys. Chem.* **1994**, *98*, 10017.

17. (a) Pérez-Casany, M.; Sánchez-Marín, J.; Nebot-Gil, I. *J. Am. Chem. Soc.* **2000**, *122*, 11585. (b) Pérez-Casany, M.; Nebot-Gil, I.; Sánchez-Marín, J. *J. Phys. Chem. A* **2000**, *104*, 6277, 10721, 11340. (c) King, M.D.; Canosa-Mas, C.E.; Wayne, R.P. *Phys. Chem. Chem. Phys.* **1999**, *1*, 2231, 2239. (d) Martínez E.; Cabañas, B.; Aranda, A.; Martín, P; Salgado, S. *J. Atmos. Chem.* **1999**, *33*, 265. (e) Martínez E.; Cabañas, B.; Aranda, A.; Martín, P; Salgado, S. *J. Phys. Chem. A* **1999**, *103*, 5321. (f) Fantechi, G.; Jensen, N.R.; Hjorth, J.; Peeters, J. *Atmos. Environ.* **1998**, *32*, 3547. (g) Pérez-Casany, M.; Nebot-Gil, I.; Sánchez-Marín, J. *J. Org. Chem.* **1998**, *63*, 6978. (h) Chew, A.A.; Atkinson, R.; Aschmann, S.M *J. Chem. Soc. Faraday Trans.*, **1998**, *94*, 1083. (i) Noremsaune, I.M.W.; Langer, S.; Ljungström, E.; Nielsen, C.J. *J. Chem. Soc. Faraday Trans.* **1997**, *93*, 525. (j) Hallquist, M.; Langer, S.; Ljungström, E.; Wängberg, I. *Int. J. Chem. Kinetics* **1996**, *28*, 467. (k) Martínez E.; Cabañas, B.; Aranda, A.; Wayne, R.P. *J. Chem. Soc. Faraday Trans.*, **1996**, *92*, 53, 4385. (l) Berndt, T; Boge, O. *J. Atmos. Chem.* **1995**, *21*, 275. (m) Galan, B.C.; Marston, G.; Wayne, R.P. *J. Chem. Soc. Faraday Trans.* **1995**, *91*, 1185. (n) Skov, H.; Benter, T.; Schindler, R.N.; Hjorth, J.;

Restelli, G. *Atmosph. Environ.* **1994**, *28*, 1583. (o) Grosjean, D.; Williams, E. *Atmos. Environ.* **1992**, *26A*, 1395.

18. (a) Langer, S.; Ljungström, E. *Int. J. Chem. Kinetics* **1994**, *26*, 367. (b) Langer, S.; Ljungström, E. *J. Chem. Soc. Faraday Trans.* **1995**, *91*, 405.

19. (a) Cabañas, B.; Salgado, S.; Martín, P; Baeza, M.T.; Martínez E. *J. Phys. Chem. A* **2001**, *105*, 4440. (b) Papagni, C; Arey, J.; Atkinson, R. *Int. J. Chem. Kinetics* **2000**, *32*, 79. (c) Ullerstam, M.; Langer, S.; Ljungström, E. *Int. J. Chem. Kinetics* **2000**, *32*, 294. (d) Alvarado, A; Arey, J.; Atkinson, R. *J. Atmos. Chem.* **1998**, *31*, 281. (e) Glasius, M; Calogirou, A; Jensen, N.R.; Hjorth, J.; Nielsen, C.J. *Int. J. Chem. Kinetics* **1997**, *29*, 527. (f) Hallquist, M; Wängberg, I.; Ljungström, E. *Environ. Sci. Technol.* **1997**, *31*, 3166.

20. (a) Atkinson, R. *J. Phys. Chem. Ref. Data* **1991**, *20*, 459. (b) Hjorth, J.; Ottobrini, G.; Restelli, G. *J. Phys. Chem.* **1988**, *92*, 2669. (c) Cantrell, C.A.; Stockwell, W.R.; Anderson, L.G.; Busarow, K.L.; Perner, D.; Schmeltekopf, A.; Calvert, J.G.; Johnston, H.S. *J. Phys. Chem.* **1985**, *89*, 139. (d) Atkinson, R.; Plum, C.N.; Carter, W.P.L.; Winer, A.M.; Pitts, J.N., Jr. *J. Phys. Chem.* **1984**, *88*, 1210, 4446 (correction).

21. (a) D'Anna, B.; Langer, S.; Ljungström, E.; Nielsen, C.J.; Ullerstam, M. *Phys. Chem. Chem. Phys.* **2001**, *3*, 1631. (b) Dlugokencky, E.J.; Howard, C.J. *J. Phys. Chem.* **1989**, *93*, 1091. (c) Morris, E.D., Jr.; Niki, H. *J. Phys. Chem.* **1974**, *78*, 1337.

22. Frisch, A.; Frisch, M.J. *Gaussian 98 User's Reference*; Gaussian Inc.: Pittsburgh, PA, p. 65, 1998.

23. Mora-Diez, N; Boyd, R.J., in preparation.

24. (a) Zhang, Q.; Bell, R.; Truong, T.N. *J. Phys. Chem.* **1995**, *99*, 592. (b) Durant, J.L. *Chem. Phys. Lett.* **1996**, *256*, 595.

25. (a) Kawaguchi, K.; Ishiwata, T.; Hirota, E.; Tanaka, I. *Chem. Phys.* **1998**, *231*, 193. (b) Wang, D.; Jiang, P.; Qian, X.; Hong, G. *J. Chem. Phys.* **1997**, *106*, 3003. (c) Ishiwata, T.; Tanaka, I.; Kawaguchi, K.; Hirota, E. *J. Mol. Spectrosc.* **1992**, *153*, 167. (d) Kawaguchi, K.; Ishiwata, T.; Tanaka, I.; Hirota, E. *Chem. Phys. Lett.* **1991**, *180*, 436. (e) Hirota, E.; Kawaguchi, K.; Ishiwata, T.; Tanaka, I. *J. Chem. Phys.* **1991**, *95*, 771. (f) Weaver, A.; Arnold, D.W.; Bradforth, S.E.; Neumark, D.M. *J. Chem. Phys.* **1991**, *94*, 1740. (g) Kawaguchi, K.; Hirota, E.; Ishiwata, T.; Tanaka, I. *J. Chem. Phys.* **1990**, *93*, 951. (h) Friedl, R.R.; Sander, S.P. *J. Phys. Chem.* **1987**, *91*, 2721. (i) Ishiwata, T.; Tanaka, I.; Kawaguchi, K.;

Hirota, E. *J. Chem. Phys.* **1985**, *82*, 2196. (j) Reuveni, A.; Luz, Z. *J. Magn. Res.* **1976**, *23*, 271.

26. (a) Eisfeld, W.; Morokuma, K. *J. Chem. Phys.* **2000**, *113*, 5587. (b) Cao, X.Y.; Hong, G.Y.; Wang, D.X.; Li, L.M.; Xu, G.X. *Chinese J. Chem.* **2000**, *18*, 267. (c) Sherril, C.D.; Lee, M.S.; Head-Gordon, M. *Chem. Phys. Lett.* **1999**, *302*, 425. (d) Mayer, M.; Cederbaum, L.S.; Köppel, H. *J. Chem. Phys.* **1994**, *100*, 899. (e) Stirling, A.; Pápai, I.; Mink, J.; Salahub, D.R. *J. Chem. Phys.* **1994**, *100*, 2910. (f) Staton, J.F.; Gauss, J.; Bartlett, R.J. *J. Chem. Phys.* **1992**, *97*, 5554. (g) Kaldor, U. *Chem. Phys. Lett.* **1991**, *185*, 131. (h) Kaldor, U. *Chem. Phys. Lett.* **1990**, *166*, 599. (i) Ishiwata, T.; Fujiwara, L.; Nagure, Y.; Obi, K.; Tanaka, I. *J. Phys. Chem.* **1983**, *87*, 1349. (j) Lund. A.; Thuomas, K.-Å. *Chem. Phys. Lett.* **1976**, *44*, 569.

27. (a) Crawford, T.D.; Lee, T.J.; Handy, N.C.; Schaefer III, H.F. *J. Chem. Phys.* **1997**, *107*, 9980. (b) Eriksson, L.A.; Wang, J.; Boyd, R.J.; Lunell, S. *J. Phys. Chem.* **1994**, *98*, 792. (c) Staton, J.F.; Gauss, J.; Bartlett, R.J. *J. Chem. Phys.* **1991**, *94*, 4084. (d) Boehm, R.C.; Lohr, L.L. *J. Comp. Chem.* **1991**, *112*, 119. (e) Morris, V.R.; Bhatia, S.; Hall, J.H., Jr. *J. Phys. Chem.* **1991**, *95*, 9203. (f) Kim, B.; Hammond, B.L.; Lester, W.A., Jr.; Johnston, H.S. *Chem. Phys. Lett.* **1990**, *168*, 131. (g) Morris, V.R.; Bhatia, S.; Hall, J.H., Jr. *J. Phys. Chem.* **1990**, *94*, 7414. (h) Boehm, R.C.; Lohr, L.L. *J. Phys. Chem.* **1989**, *93*, 3430. (i) Davy, R.D.; Schaefer III, H.F. *J. Chem. Phys.* **1989**, *91*, 4410. (j) Kim, B.; Johnston, H.S.; Clabo, D.A., Jr.; Schaefer III, H.F. *J. Chem. Phys.* **1988**, *88*, 3204. (k) Siegbahn, P.E.M. *J. Comput. Chem.* **1985**, *6*, 182. (l) Baird, N.C.; Taylor, K.F. *Chem. Phys. Lett.* **1981**, *80*, 83. (m) Dewar, M.J.S.; Rzepa, H.S. *J. Am. Chem. Soc.* **1978**, *100*, 784. (n) Olsen, J.F.; Burnelle, L. *J. Am. Chem. Soc.* **1970**, *92*, 3659. (o) Chantry, G.W.; Horsfeld, A.; Morton, J.R.; Wiffen, D.H. *Mol. Phys.* **1962**, *5*, 589.

28. (a) Löwdin, P.-O. *Rev. Mod. Phys.* **1963**, *35*, 496. (b) Löwdin, P.-O. *Adv. Chem. Phys.* **1969**, *14*, 283.

29. Johnson, B.G.; González, C.A.; Gill, P.M.W.; Pople, J.A. *Chem. Phys. Lett.* **1994**, *221*, 100.

30. Kestner, N.R.; Combariza, J.E. in *Reviews in Computational Chemistry*, Volume 13, Lipkowits, K.B. and Boyd, D.B., Editors, Wiley-VCH, New York, p. 99, 1999.

31. (a) Boys, S.F.; Bernardi, F. *Mol. Phys.* **1970**, *19*, 553. (b) Handy, N.C.; Pople, J.A.; Shavitt, I. *J. Phys. Chem.* **1996**, *100*, 6007 (This paper gives a biographical synopsis on Boys's work). (c) Jansen, H.B.; Ros, P. *Chem. Phys. Lett.* **1969**, *3*, 140.

32. Benson, S.W. *Thermochemical Kinetics*, 2nd Ed., Wiley & Sons, New York, p. 43, 1976.

33. Chuang, Y-Y; Truhlar, D.G. *J. Chem. Phys.* **2000**, *112*, 1221.

34. (a) Galano, A.; Alvarez-Idaboy, J.R.; Montero, L.A.; Vivier-Bunge, A. *J. Comp. Chem.* **2001**, *22*, 1138. (b) Alvarez-Idaboy, J.R.; Mora-Diez, N.; Boyd, R.J.; Vivier-Bunge, A. *J. Am. Chem. Soc.*, **2000**, *122*, 3715.

35. Mora-Diez, N.; Boyd, R.J. *J. Phys. Chem.*, **2001**, submitted.